Absorption and Fluorescence Spectra of Heterocyclic Isomers from Long-Range-Corrected Density Functional Theory in Polarizable Continuum Approach

ARTICLE *in* THE JOURNAL OF PHYSICAL CHEMISTRY A · FEBRUARY 2012

Impact Factor: 2.69 · DOI: 10.1021/jp300305j · Source: PubMed

1 AUTHOR:

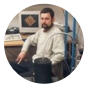

Andriy V. Kityk
Czestochowa University of Technology
206 PUBLICATIONS **1,935** CITATIONS

SEE PROFILE

THE JOURNAL OF PHYSICAL CHEMISTRY A

Article

pubs.acs.org/JPCA

Absorption and Fluorescence Spectra of Heterocyclic Isomers from Long-Range-Corrected Density Functional Theory in Polarizable Continuum Approach

Andriy V. Kityk*

Faculty of Electrical Engineering, Czestochowa University of Technology, Al. Armii Krajowej 17, 42-200 Czestochowa, Poland

ABSTRACT: Long-range-corrected (LC) DFT/TDDFT methods may provide adequate description of ground and excited state properties; however, accuracy of such an approach depends much on a range separation (exchange screening) representing adjustable model parameter. Its relation to a size or specific of molecular systems has been explored in numerous studies, whereas the effect of solvent environment is usually ignored during the evaluation of state properties. To benchmark and assess the quality of the LC-DFT/TDDFT formalism, we report the optical absorption and fluorescence emission energies of organic heterocyclic isomers, DPIPQ and PTNA, calculated by LC-BLYP DFT/TDDFT method in the polarizable continuum (PCM) approach. The calculations are compared with the optical absorption and fluorescence spectra measured in organic solvents of different polarity. Despite a considerable structural difference, both dyes exhibit quite similar range separations being somewhat different for the optical absorption and fluorescence emission processes. Properly parametrized LC-BLYP xc-potential well reproduces basic features of the optical absorption spectra including the electronic transitions to higher excited states. The DFT/TDDFT/PCM analysis correctly predicts the solvation trends although solvatochromic shifts of the electronic transition energies appear to be evidently underestimated in most cases, especially for the fluorescence emission. Considering the discrepancy between the experiment and theory, evaluated state dipole moments and solvation corrections to the exchange screening are analyzed. The results of the present study emphasize the importance of a solvent-dependent range separation in DFT/TDDFT/PCM calculations for investigating excited state properties.

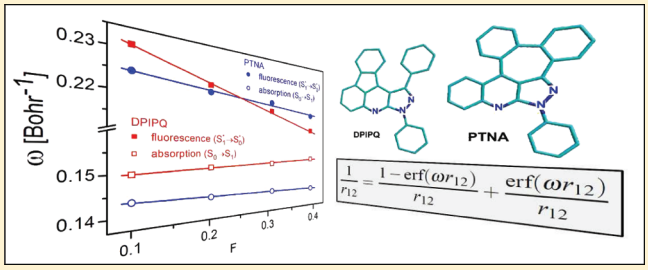

1. INTRODUCTION

Heterocyclic organic compounds attract significant attention due to growing number of their applications in organic electronics and/or optoelectronics, mainly as materials used in production of organic field-effect transistors,[1,2] light emitting diodes and electroluminescence displays,[3−7] photovoltaic devices,[8,9] dye lasers,[10,11] etc. The basic idea behind the investigations usually lies in a search of new organic dyes that exhibit full color gamut, high fluorescence efficiency and quantum yield, tunable emission wavelength, or bandwidth. Due to this reason their electronic properties in relation to a molecular structure, chemical substitution or solvent environment appear in a scope of numerous experimental and theoretical studies where the optical spectroscopy techniques are usually combined with a quantum chemical analysis or modeling.[12−19]

Recent progress in the heterocycle organic chemistry has resulted in development of novel annulated analogues of azafluoranthenes and azulenes[20−24] representing the heterocyclic five- and seven-membered regioisomers, respectively. Similar organic materials were originally of interest for pharmacology, as efficient tissues oxygenators and antidepressant agents,[25,26] or biotechnology compounds used for binding of macromolecules, particularly as efficient DNA intercalators.[27,28] However, quite recent spectroscopic studies have revealed that such heterocyclic isomers may be also considered as novel efficient dyes for luminescent or electroluminescent applications in green-yellow region of the visible spectra.[7,29] The annulated azafluoranthene and azulene dyes were originally synthesized by Danel and co-workers[20] from triphenylpyrazoloquinoline derivatives. Pirazoloquinolines itself are known as efficient fluorescent and electroluminescent materials preferably in blue, rarely blue-green regions of the visible spectra.[4−6,30−32] Cyclization of triphenylpirazoloquinoline derivatives into the five or seven-membered heterocyclic regioisomers provides a significant red shift of the emission and first absorption bands[23] that may be of interest for a number of applications. In the polar environment such dyes exhibit an opposite solvatochromism, i.e., the hypsochromic (blue) shift of the first absorption band and the bathochromic (red) shift of the fluorescence emission. Such trends have been successfully explained within several approaches, particularly by a simple Onsager reaction field model based on semiempirical calculations (PM3 method)[21,22] and, later on, by DFT/TDDFT applying the hybrid exchange−correlation (xc) potential B3LYP in combination with the polarizable

Received: January 10, 2012
Revised: February 15, 2012
Published: February 22, 2012

continuum model (PCM).[33,33] In both cases relevant interpretation refers to a specific orientation of the ground and excited state dipole moments. Moreover, the B3LYP/PCM method quite accurately predicts the excitation energy of the $S_0 \rightarrow S_1$ transition and gives a reasonable value for its solvatochromic shift. Nevertheless, an evident failure occurs if the emission energy associated with the reverse $S_1 \rightarrow S_0$ transition is evaluated. Surprisingly, but already in the gas phase, the TDDFT/B3LYP approach considerably underestimates the emission energy giving an error of 0.4−0.7 eV, which further increases in polar solvent environment. Analysis of such a discrepancy should consider specific features of the hybrid xc-potential B3LYP used in TDDFT calculations. Despite its popularity in organic chemistry, several critical issues were addressed in respect to this method; see ref 17 and references therein. It turns out that TDDFT/B3LYP usually underestimates the excitation energies, especially if one deals with the charge transfer (CT) states[35] or large-sized molecules.[36,37] But recent experience even with midsized molecules, such as, e.g., heterocyclic azafluoranthenes or azulenes,[33,33] shows that this hybrid method appears also not very suitable for the geometry optimization in the excited state(s), which particularly explains large errors in computed fluorescence emission energies.

The reason for such discrepancies is usually addressed to the fact that B3LYP does not account for the long-range interactions. Applying so-called long-range-corrected (abbreviated as LC or LRC in the literature) approaches, as, e.g., LC-BLYP, may considerably improve the accuracy of the DFT/TDDFT calculations. Introduced originally by Savin[38] and Gill,[39] this method has been developed in a number of later works.[40−48] In contrast to conventional hybrid functionals incorporating a constant fraction of HF exchange, the LC methods mix HF exchange densities nonuniformly by partitioning the electron repulsion operator on a short-range interaction, which decays rapidly on a length scale $\propto \omega^{-1}$, and the long-range part of the Coulomb interaction. Here ω is the range-separation (screening exchange) parameter that is sensitive to the size of the molecule and is specific for the electron density distribution. In a more explicit characterization ω should be considered as a functional of the density $\rho(\vec{r})$,[49] which has been demonstrated for the homogeneous electron gas; see, e.g., refs 50 and 51. Several approximations for $\omega(\rho(\vec{r}))$ have been indeed developed in refs 50 and 52, but they fail to preserve the size consistency in the exchange−correlation interactions. For moderately large organic chromophores it was proved explicitly[53] that there is no value of ω that is simultaneously optimal (or nearly optimal) both for ground state properties, such as atomization energies or reaction barrier heights, and for excited state properties or vertical excitation energies describing the electronic transitions between these states. Due to this reason the exchange screening parameter ω should be considered rather as a model parameter being adjustable for a particular molecular system, electronic state(s) or transition(s) subjected to analysis.

In this work, we explore the absorption and fluorescence from the LC-BLYP DFT/TDDFT method in PCM approach for a pair of the heterocyclic dyes. The actual study deals with the diphenyl derivative of annulated azafluoranthene (1,3-diphenyl-3*H*-indeno[1,2,3-*de*]pyrazolo[3,4-*b*]quinoline, abbreviated hereafter as DPIPQ) and the phenyl derivative of annulated heteroazulene (6-phenyl-6*H*-5,6,7-triazadibenzo[*f*,*h*]-naphtho[3,2,1-*cd*]azulene, hereafter PTNA) representing the five- and seven-membered heterocyclic isomers, respectively, with the chemical structure as shown below.

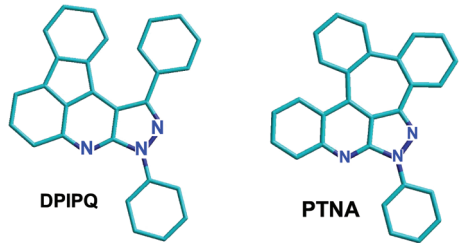

Both molecules of similar size and with identical chemical formulas ($C_{28}H_{17}N_3$) exhibit considerably different structures. Such a choice is made intentionally to study how the isomeric structural modification and solvation influence the range separation and the performance of LC-BLYP xc-potential in DFT/TDDFT/PCM calculations. For this reason the results of calculations are compared with measured optical absorption and fluorescence spectra of these heterocyclic dyes reported in a series of recent works.[22,33,34]

2. METHODOLOGY AND COMPUTATIONAL DETAILS

In the LC methods the two-electron repulsion operator $1/r_{12}$ is divided into short- and long-range parts by means of Ewald-style partition based on the error function (erf)[45−48]

$$\frac{1}{r_{12}} = \frac{1 - \mathrm{erf}(\omega r_{12})}{r_{12}} + \frac{\mathrm{erf}(\omega r_{12})}{r_{12}} \quad (1)$$

where $r_{12} = |\mathbf{r}_2 - \mathbf{r}_1|$ is the distance between the electrons at the coordinate vectors $\mathbf{r}_1$ and $\mathbf{r}_2$. Here the exchange screening parameter ω, expressed in units of Bohr^{-1}, determines the ratio between the two ranges depending on the value of r_{12}. The first term in eq 1 is a short-range interaction described by DFT exchange potential, which decays rapidly on a length scale of $2/\omega$, and the second term is the long-range interaction described by the HF exchange integral. In the present study we use pure DFT xc-potential BLYP and thus the exchange−correlation energy according to the LC scheme is given as

$$E_{xc} = E_{c,LYP} + E^{SR}_{x,B88} + E^{LR}_{x,HF} \quad (2)$$

where $E_{c,LYP}$ is the Lee−Yang−Parr correlation functional[54] in its original DFT definition, $E^{SR}_{x,B88}$ is the short-range part of the Becke's exchange energy,[55] and $E^{LR}_{x,HF}$ is the HF contribution to exchange computed with the long-range part of the Coulomb operator. In contrast to the xc-potentials of conventional DFT methods, which exhibit a wrong asymptotic behavior, the exchange potential of LC methods recovers the exact $1/r$ dependence at large interelectronic distances. It is particularly important for the charge transfer processes, because the excitations of that type are especially sensitive to the asymptotic part of the nonlocal xc-potential.

The DFT calculations have been performed using the quantum chemical package of programs Gaussian-09[56] choosing LC-BLYP method with the standard 6-31+G(d,p) basis set. To explore the influence of range-separated exchange on absorption and emission spectra of the heterocyclic dyes, the original xc-potential LC-BLYP (ω = 0.47 Bohr^{-1}) has been reparameterized by varying the exchange screening parameter ω in the range 0.07−0.35 Bohr^{-1}. For each particular ω-value we have performed the calculations on a full absorption−emission cycle including the DFT geometry optimization in the

dx.doi.org/10.1021/jp300305j | J. Phys. Chem. A 2012, 116, 3048−3055

singlet ground state S_0 ⇒ TDDFT calculation of vertical excitation energies from the ground state ($S_0 \rightarrow S_i$ transitions, i = 1−49) ⇒ TDDFT geometry optimization in the lowest singlet excited state (molecular geometry relaxation $S_1 \rightarrow S_1^*$) ⇒ TDDFT calculation of the emission energy corresponding to the vertical transition from the lowest excited state ($S_1^* \rightarrow S_0^*$ transition). Herewith the star (*) superscript indicates that a relevant state is characterized by the equilibrium excited state geometry. Otherwise, the equilibrium molecular geometry corresponds to the ground state. To account for the solvation, the TDDFT calculations have been combined with PCM available in Gaussian-09 using the linear response (LR) or state specific (SS) approaches as for the excitation or emission processes, respectively. The geometrical optimization has been performed by the DFT/PCM (ground state S_0) or TDDFT/PCM (excited state S_1) methods, both in the LR approach.

3. RESULTS AND DISCUSSION

In this section we explore the absorption and emission energies of PTNA and DPIPQ dyes calculated by TDDFT/PCM method in different solvents. The solvent polarity is expressed by means of Lippert−Mataga polarity function,[57,58] $F(\varepsilon,n) = (\varepsilon - 1)/(2\varepsilon + 1) - (n^2 - 1)/(4n^2 + 2)$, where ε is the static dielectric constant and n is the refractive index of the solvent. The relevant model assumes a point dipole situated in the center of the spherical cavity and neglects the mean solute polarizability in the states involved in the electronic transitions. It particularly differs from existing alternative definitions, such as, e.g., the McRae polarity function[59] in the model accounting the solute polarizability effects. However, it should be emphasized explicitly that the form of the F function is of marginal meaning in actual study because it has no impact on the DFT/TDDFT/PCM calculations and serves for a quantitative characterization of the solvent polarity only. In our calculations we refer to three solvents, weakly polar cyclohexane (CHX, F = 0.1007), medium polar tetrahydrofuran (THF, F = 0.3084), and highly polar acetonitrile (ACN, F = 0.3928). Such a choice is relevant to recent experimental studies on PTNA[34] and DPIPQ[33] dyes where the optical absorption and fluorescence spectra were measured for the same set of the solvents. The open symbols in Figure 1a,b are the experimental data points taken directly from these works which represent the energies of the vertical optical absorption ($S_0 \rightarrow S_1$, 0 → 0′ transition, marked by circles) and fluorescence emission ($S_1^* \rightarrow S_0^*$, 0′ → 0 transition, marked by squares). As the solvent polarity rises, both dyes exhibit the blue shift of the first absorption band and the red shift of the fluorescence band. An interpolation of these dependences (see broken lines in Figure 1a,b) gives the excitation or emission energy in the mid of the F range, i.e., for a hypothetic generic solvent (abbreviated hereafter as GS, $F = F_{GS}$ = 0.2026, ε = 3.3, $\varepsilon_\infty = n^2$ = 2.0). Accordingly, the data points marked by the star symbol in Figure 1a,b correspond to the excitation or emission energies of the DPIPQ or PTNA dyes in the GS. Those interpolated values have been used as the reference ones for the reparametrization of LC-BLYP xc-potential.

Panels a and b of Figure 2 show the singlet excitation ($E_{S_0 \rightarrow S_1}$) and emission ($E_{S_1^* \rightarrow S_0^*}$) energies vs ω being calculated in the GS for DPIPQ and PTNA dyes, respectively. Both energies rise with the separation parameter ω, which is typical for such type of the xc-potential. In the case of the PTNA dye the singlet excitation (emission) consists mainly of the HOMO ⇆ LUMO

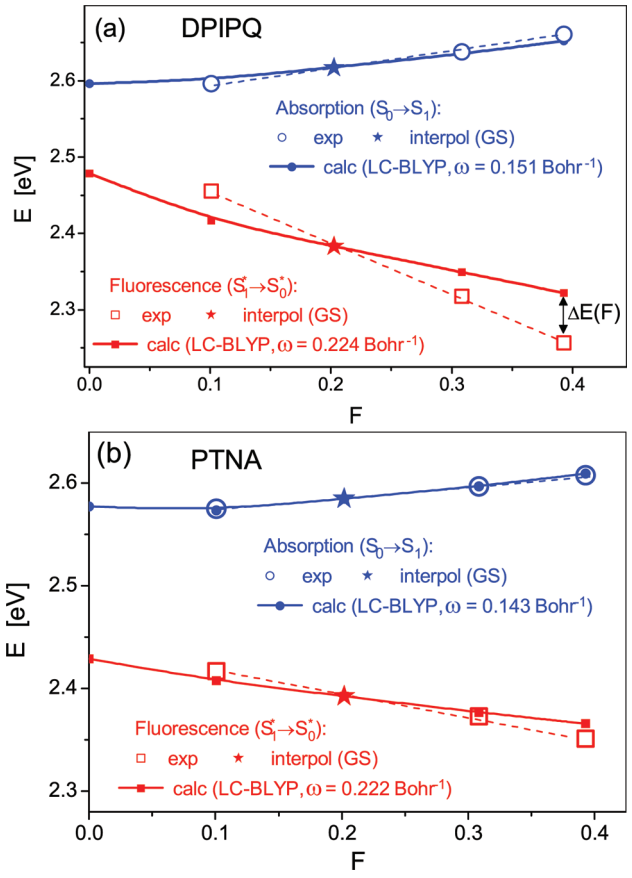

Figure 1. Optical absorption [$S_0 \rightarrow S_1$ (0 → 0′) transition, blue circles] and fluorescence emission [$S_1^* \rightarrow S_0^*$ (0′ → 0) transition, red squares] energies vs the solvent polarity F for DPIPQ (a) and PTNA (b) dyes. Solid symbols represent values computed within LC-BLYP DFT/TDDFT/PCM approach. Open symbols are the experimental data points taken from refs 33 and 34. Star symbols mark interpolated values (see broken lines) corresponding to hypothetic GS ($F = F_{GS}$ = 0.2026, ε = 3.3, $\varepsilon_\infty = n^2$ = 2.0) being used for ω-parametrization of the LC-BLYP xc-potential (see labeled ω-values as for the absorption and emission processes being parametrized for GS).

transition although its contribution slightly decreases while ω rises, namely from 97%(98%) at ω = 0.07 Bohr^{-1} to 92%(95%) at ω = 0.35 Bohr^{-1}, respectively. The HOMO → LUMO transition appears to be dominant also in the origin of the first absorption band of DPIPQ dye but its contribution more strongly depends on the range separation decreasing from about 96% (ω = 0.07 Bohr^{-1}) to 72% (ω = 0.35 Bohr^{-1}). For its expense other contributions, HOMO−1 → LUMO, HOMO−2 → LUMO, and HOMO−3 → LUMO, become more evident at larger ω; particularly at ω = 0.35 Bohr^{-1} they contribute into the electronic $S_0 \rightarrow S_1$ transition by about 11%, 3%, and 6%, respectively. The situation is considerably different for the fluorescence emission of DPIPQ. At ω < 0.24 Bohr^{-1} the vertical emission from the lowest excited state is caused mainly by the HOMO ← LUMO transition (>91%) whereas at higher range separations (ω > 0.25 Bohr^{-1}) the HOMO−1 ← LUMO transition becomes suddenly dominant, above 76%. Accordingly, the data points that represent the emission energy of DPIPQ are marked in Figure 2a by different symbols to emphasize considerably different properties of the fluorescent emission at ω < 0.24 Bohr^{-1} and ω > 0.25 Bohr^{-1}, respectively. The horizontal broken lines, marked by blue or red in Figure

dx.doi.org/10.1021/jp300305j | J. Phys. Chem. A 2012, 116, 3048−3055

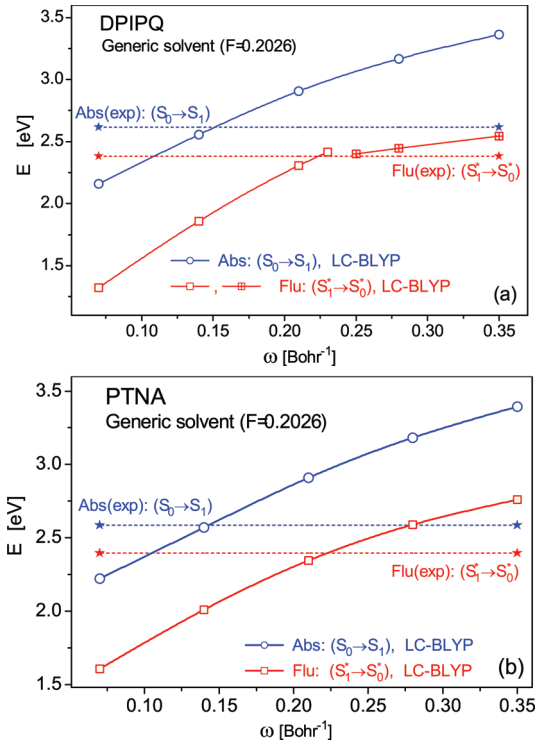

Figure 2. Optical absorption [$S_0 \rightarrow S_1$ ($0 \rightarrow 0'$) transition, blue circles] and fluorescence emission [$S_1^* \rightarrow S_0^*$ ($0' \rightarrow 0$) transition, red squares] energies vs the range separation parameter ω computed within LC-BLYP DFT/TDDFT/PCM approach in GS for DPIPQ (a) and PTNA (b) dyes. Horizontal broken lines with the star symbol ends are the optical absorption (blue) and fluorescence emission (red) energies in GS being determined by interpolation of the experimental data (Figure 1). Their intersection with corresponding calculated $E_{S_0 \rightarrow S_1}(\omega)$ or $E_{S_1^* \rightarrow S_0^*}(\omega)$ curves give the magnitudes of the range separation parameter ω in GS, as labeled in Figure 1.

2a,b, correspond to the excitation ($S_0 \rightarrow S_1$, $0 \rightarrow 0'$ transition) or emission ($S_1^* \rightarrow S_0^*$, $0' \rightarrow 0$ transition) energies in the GS for DPIPQ and PTNA dyes, respectively. Their intersection with the calculated $E_{S_0 \rightarrow S_1}(\omega)$ or $E_{S_1^* \rightarrow S_0^*}(\omega)$ curves give the magnitude of the range separation for LC-BLYP xc-potential which provide exact (errorless) transition energy in each of those particular cases. It turns out that for the vertical absorption ($S_0 \rightarrow S_1$) the parameter ω takes only slightly different values for both dyes, namely 0.151 Bohr^{-1} for DPIPQ and 0.143 Bohr^{-1} for PTNA. For the fluorescence emission, which represents the inverse electronic $S_1^* \rightarrow S_0^*$ transition, corresponding values are even closer, 0.224 Bohr^{-1} for DPIPQ and 0.222 Bohr^{-1} for PTNA, despite the fact that these isomers are indeed characterized by considerably different molecular structures. Thus, LC-BLYP calculations for DPIPQ and PTNA molecules indicate relatively long-range-separation for both absorption and emission processes. It may seem to be a little unusual but not too surprising, although ω-values are evidently smaller here than the conventional magnitude 0.33 Bohr^{-1} suggested by Iikura et al.[41] For instance, a study on coumarins[60] and porphyrins[61] using LC-BLYP xc-potential indicated that the optimized value of ω is 0.17 Bohr^{-1}. Long range separations ($\omega \sim 0.21$ Bohr^{-1}) have been also found by Balanay and Kim[62] for moderately sized molecules of tetrahydroquinoline dyes. Moreover, Rohrdanz and Herbert[53] have revealed that excited state properties are strongly ω-dependent, being considerably different for small and large molecules. It turns out that smaller values of ω are more appropriate for excitation energies in large molecules. In other words, ω^{-1} should be roughly comparable to their size, which enables the short-range Coulomb operator to fully decay to zero on the length scale of the molecule. A detailed discussion on this issue may be found in ref 60. On the other hand, it must be emphasized explicitly that the small ω-values in the case of DPIPQ or PTNA molecules are basically not due to the solvent effect, despite the fact that the solvent environment has a certain impact on its magnitude. However, its influence is indeed small, as will be shown below; corresponding corrections for these dyes do not exceed 0.005−0.01 Bohr^{-1} in the entire region of solvent polarities.

A more challenging question is obviously a distinct difference in the ω-value if one switches from the optical absorption to fluorescence emission or vice versa. Assuming, e.g., that the LC-BLYP xc-potential is parametrized by adjusting the range separation for the optical absorption, the error in a predicted emission energy then is about 0.45 eV for DPIPQ or 0.37 eV for PTNA. Thus, the discrepancy in both cases is comparable to the one obtained in TDDFT calculations using the hybrid B3LYP xc-potential.[33,33] Basically, nothing special would be in this fact taking into account that the parameter ω in LC-BLYP method should be considered as a functional of the density $\rho(\vec{r})$;[49,53] thus, a geometrical rearrangement (conformational relaxation) accompanying the absorption−emission circle requires in principle the readjustment of the exchange screening individually for the absorption and emission processes. However, it is somewhat astonishing that a switching between considerably different molecular structures, as, e.g., DPIPQ and PTNA isomers, requires only a minor modification of the ω-value if one deals with either absorption or emission processes. Nevertheless, a properly parametrized LC-BLYP xc-potential reasonably predicts the excitation energies and oscillator strengths, including the ones related to higher excited states. Thereby, the basic features of the optical absorption spectra for these dyes may be well reproduced; see Figure 3a,b. One should notice that the first absorption maximum appears for both dyes in the region 452−454 nm whereas the vibronic $0 \rightarrow 0'$ transition relevant with the first absorption band, L_1, indeed should be assigned to the kink-like shoulder observed at its red wing, i.e., at about 478 nm (2.594 eV) for DPIPQ and 481 nm (2.578 eV) for PTNA, as marked by arrow in Figure 3a,b, respectively. Accordingly, the spectral position of the first vibronic band rather than the position of the first absorption maximum is relevant for further comparison with theoretical calculations. The continuous lines in Figure 3a,b are the optical absorption spectra calculated within the DFT/TDDFT/PCM approaches based on the pure LC-BLYP [blue, ω = 0.151 Bohr^{-1} (DPIPQ) and ω = 0.143 Bohr^{-1} (PTNA)] or hybrid B3LYP [red] xc-potentials. The absorption bands are modeled here by the Gaussian function with the FWHM of 0.3 eV (DPIPQ) or 0.33 eV (PTNA), which most properly describes actual band shape broadening. Further methodology details regarding such calculations can be found in ref 21−23 and 29. The combined DFT/TDDFT/PCM/LC-BLYP calculations exhibit evidently better performance compared to the ones based on the hybrid xc-potential B3LYP. Particularly, the spectral position of the first absorption band, L_1, for both isomers in CHX solution is predicted by the DFT/TDDFT/PCM/LC-BLYP approach with an accuracy better than 0.005 eV. The error is obviously larger for the higher energy states. Particularly, the excitation energies relevant to the strongest

dx.doi.org/10.1021/jp300305j | J. Phys. Chem. A 2012, 116, 3048−3055

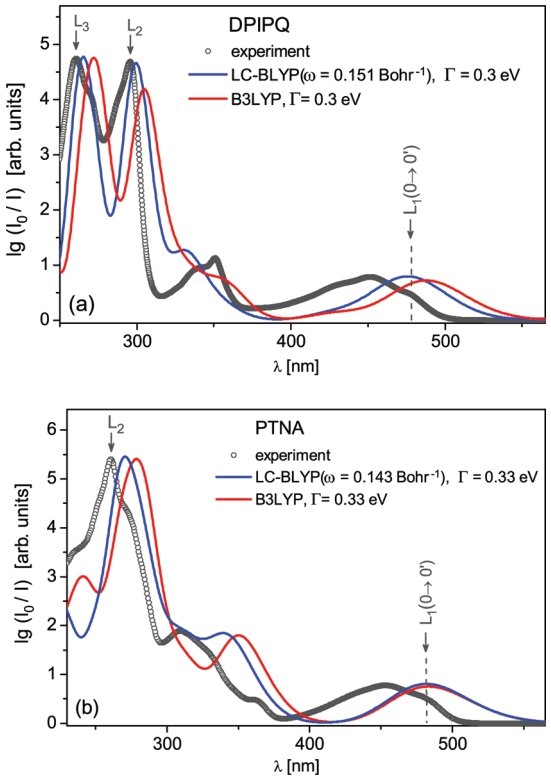

Figure 3. Optical absorption spectra of DPIPQ (a) and PTNA (b) dyes in CHX solution. Open symbols represent the measured spectra.[33,34] Solid lines correspond to the spectra computed within the DFT/TDDFT/PCM approaches based on hybrid B3LYP (red) and pure LC-BLYP (blue) xc-potentials.

absorption bands, L_2 and L_3 of DPIPQ (Figure 3a) or the absorption band L_2 of PTNA (Figure 3b), are underestimated by about 0.06 or 0.17 eV, respectively, but even in these cases the relative error is less than 4%. For comparison, the DFT/TDDFT/PCM/B3LYP approach gives in most cases nearly a twice larger error in evaluation of the same excitation energies.

Another challenging question is an influence of the solvent environment on the electron density and related to it range separation in LC DFT/TDDFT methods. Actual work explores this problem by presenting the results of DFT/TDDFT/PCM calculations in solvents of different polarities and comparing them with the experimental data; see Figure 1a,b. Notice again that in our analysis the LC-BLYP xc-potential have been parametrized individually for the optical absorption [ω = 0.224 Bohr^{-1} (DPIPQ) or 0.222 Bohr^{-1} (PTNA)] and fluorescence emission [ω = 0.151 Bohr^{-1} (DPIPQ) or 0.143 Bohr^{-1} (PTNA)] processes, which provides errorless excitation or emission transition energies for each molecule in the GS ($F = F_{GS}$); see the star symbols that appear at the intersection of the interpolated measured and calculated $E(F)$ dependences. Accordingly, any analysis makes sense only away from this region, i.e., at $F < F_{GS}$ or $F > F_{GS}$. The most appropriate and simplest way is a comparison of the measured and calculated solvatochromic slopes. In all the cases DFT/TDDFT/PCM analysis properly predicts its sign being relevant with the blue shift of the first absorption band and the red shift of the fluorescence band on the rising solvent polarity F. For PTNA molecules the excitation energies calculated in different solvents result to the solvatochromic slope $dE_{S_0\rightarrow S_1}/dF$ equals 0.121 eV. This magnitude only a bit exceeds the experimental value 0.11 eV; i.e., the discrepancy practically lies within an experimental error of ~0.01 eV. On the other hand, the absolute value of the solvatochromic slope corresponding to the emission energy appears to be considerably underestimated for this dye: −0.145 eV (calculation) compared to −0.22 eV (experiment). For DPIPQ molecules the discrepancy between the experiment and theory is even larger. DFT/TDDFT/PCM calculations provide in both cases evidently underestimated solvatochromic shifts with relevant slopes $dE_{S_0\rightarrow S_1}/dF$ = 0.174 eV (optical absorption) and $dE_{S_1^*\rightarrow S_0^*}/dF$ = −0.324 eV (fluorescence emission). For comparison, the slope values derived from the measured spectra in these cases are 0.22 eV and −0.6774 eV, respectively. What could be the reasons for such discrepancy? Thinking of the PCM model, which represents a self-consistent reaction field (SCRF) approach, the solvatochromic shift is caused by the reaction field induced in a solvent by a solute. For this reason the dipole moments in the ground $\vec{\mu}_0 = \vec{\mu}(S_0)$ [$\vec{\mu}_0^* = \vec{\mu}(S_0^*)$] and excited $\vec{\mu}_1 = \vec{\mu}(S_1)$ [$\vec{\mu}_1^* = \vec{\mu}(S_1^*)$] states have direct impact on the electronic transition energies. Particularly, in the simplest Onsager reaction field (ORF) approach, which replaces a set of overlapping cavity spheres used in PCM by just a single spherical cavity, the solvatochromic shift of the absorption (ΔE_a) or emission (ΔE_f) energies is defined by the Lippert−Mataga equations,[57,58] $\Delta E_a \approx -2\vec{\mu}_0(\vec{\mu}_1 - \vec{\mu}_0)a_0^{-3}F$ and $\Delta E_f \approx -2\vec{\mu}_1^*(\vec{\mu}_1^* - \vec{\mu}_0^*)a_0^{-3}F$, respectively. Here a_0 is the effective cavity (Onsager) radius; being a crude parameter of ORF model, its choice has a direct impact on the solvatochromic correction into the excitation or emission energies. A similar remark may be addressed to PCM approach, for which the results of calculations indeed depend on how the solute spherical cavities are defined. Their improper choice may lead to solvation energy corrections being either underestimated or overestimated simultaneously for both absorption and emission processes. Evidently, it is not the case of actual heterocyclic isomers, especially PTNA, for which the solvatochromic shift is considerably underestimated for the fluorescence emission and, at the same time, slightly overestimated for the optical absorption. Another reason explaining the discrepancy between the experiment and theory could be evaluated ground and excited state dipole moments that are expected to be underestimated in DFT/TDDFT calculations using LC-BLYP xc-potential. This seems to be possible if we compare the results of present calculations with the ones obtained in refs 33 and 34 using the hybrid B3LYP potential. For the fluorescence emission in the gas phase, the DFT/TDDFT/LC-BLYP method gives the ground (μ_0^*) and the lowest excited state (μ_1^*) dipole moments equal to 3.77 and 2.23 D for PTNA and 3.47 and 4.69 D for DPIPQ, respectively. In comparison, the B3LYP method provides larger state dipole moments, namely 4.16 and 4.03 D for PTNA and 3.99 and 8.16 D for DPIPQ, respectively. Accordingly, the solvatochromic shift of the fluorescence emission in the hybrid B3LYP method is at least twice as large compared to the one based on LC-BLYP potential. Although such justification seems quite plausible, there is room for alternative explanations. First of all, one must emphasize the fact that the absorption−emission cycle, $S_0 \rightarrow S_1 \rightarrow S_1^* \rightarrow S_0^* \rightarrow S_0$, is accompanied by the solute−solvent reorganization caused by the conformational relaxation and reorientation of solvent molecules when switching from the absorption to emission processes ($S_1 \rightarrow S_1^*$ transition) or vice versa ($S_0^* \rightarrow S_0$ transition). Relevant modification in the solute electron density may be characterized

dx.doi.org/10.1021/jp300305j | J. Phys. Chem. A 2012, 116, 3048−3055

by changes in the state dipole moments; see Figure 4. For comparison, here are presented the ground and excited state

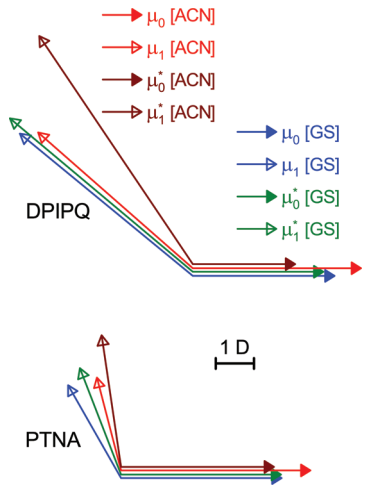

Figure 4. Ground ($\vec{\mu}_0$, $\vec{\mu}_0^*$) and excited state ($\vec{\mu}_1$, $\vec{\mu}_1^*$) dipole moments of DPIPQ and PTNA molecules computed within the LC-BLYP DFT/TDDFT/PCM approach in GS and ACN. In each case the relative spatial orientation of both dipoles is presented; i.e., the ground state dipole moment is always directed horizontally to the right whereas a relevant excited state dipole moment keeps relative to it angular orientation. Here the state dipole moments $\vec{\mu}_0$ and $\vec{\mu}_1$ correspond to the equilibrium ground state geometry [optical absorption, ω = 0.143 Bohr^{-1} (PTNA) and ω = 0.151 Bohr^{-1} (DPIPQ)] whereas the state dipole moments $\vec{\mu}_0^*$ and $\vec{\mu}_1^*$ are relevant to the equilibrium excited state geometry [fluorescence emission, ω = 0.222 Bohr^{-1} (PTNA) and ω = 0.224 Bohr^{-1} (DPIPQ)], marked by different online colors.

dipole moments calculated for DPIPQ and PTNA molecules in GS and ACN solutions. The conformational relaxation and solvent reorganization in the excited state result to recognizable changes in the state dipole moments. Already in moderately polar GS this leads to a certain increase in the ground state dipole moment ($\mu_0^* > \mu_0$) and a decrease in the excited state dipole moment ($\mu_1^* < \mu_1$) and also a decrease in the angle between these moments ($\widehat{\vec{\mu}_0^*\vec{\mu}_1^*} < \widehat{\vec{\mu}_0\vec{\mu}_1}$). In strongly polar solvents, as, e.g., ACN, such trends become even more pronounced. The blue shift of the first absorption band and the red shift of the fluorescence band upon rising solvent polarity are explained by a specific orientation of the dipole moments, i.e., appear to be consistent with the opposite signs of the scalar products $\vec{\mu}_0(\vec{\mu}_1 - \vec{\mu}_0)$ and $\vec{\mu}_1^*(\vec{\mu}_1^* - \vec{\mu}_0^*)$, as it evidently follows from the vector diagrams given in Figure 4. Solvent modified dipole moments have an obvious direct impact on the solvatochromic shift, but this effect is already accounted for within the DFT/TDDFT/PCM calculations based on a self-consistent state specific approach. Thus, the only thing left to consider is a correction to the range separation caused by the solvent effect on the solute electron density. In principle, $\omega(F)$ dependence may be determined by performing a full cycle of DFT/TDDFT/PCM calculations in the solvents of different polarities, i.e., as we did above by determining the ω-value in GS. Such a time-consuming procedure may be indeed avoided using the calculated $E(\omega)$ dependence (Figure 2) and expanding the range separation parameter in a power series, $\omega(F) = \omega^* + (\partial\omega/\partial E)\Delta E(F) + ...$, in the vicinity of $\omega^* \equiv \omega(F_{GS})$, where $\Delta E(F)$ is the discrepancy between the calculated and measured transition energies vs solvent polarity; see Figure 1a. In such evaluations we rely on the fact that the derivative $\partial\omega/\partial E \equiv (\partial E/\partial\omega)^{-1}|_{\omega=\omega^*}$ is weakly F-dependent for both dyes; i.e., its deviations do not exceed 4% (PTNA) and 8% (DPIPQ), which provides sufficiently high accuracy in the estimated ω-value, namely better than 0.001 Bohr^{-1}. Figure 5 presents $\omega(F)$ dependences corresponding to

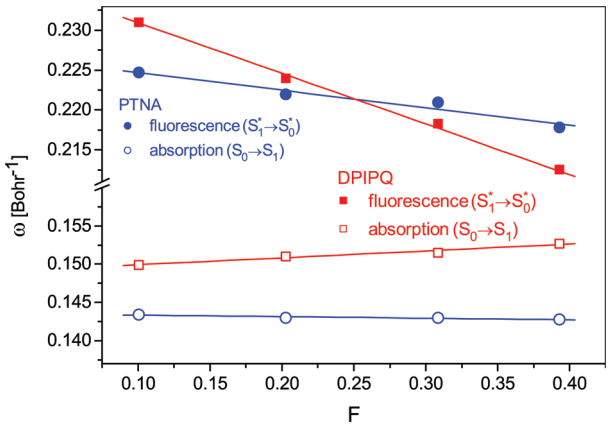

Figure 5. Range separation parameter ω vs the solvent polarity F for DPIPQ (red squares) and PTNA (blue circles) dyes. Open and solid symbols correspond to the optical absorption and fluorescence emission processes, respectively.

the absorption ($S_0 \rightarrow S_1$) and emission ($S_1^* \rightarrow S_0^*$) processes for both heterocyclic isomers. In all the cases the relative changes of ω vs F are less than 10%. However, DPIPQ exhibits considerably stronger variation of the range separation on the solvent polarity than PTNA dye, especially in the case of the fluorescence emission. Recognized trends well correlate with the solvatochromic shifts of the excitation/emission energies, which evidently are larger for the DPIPQ molecule compared to the ones for the PTNA isomer. Such correlation may be found as quite logical taking into account that an influence of solvation on the state energies as well as the solute electron density, is defined in both cases by the Onsager reaction field,[63] $\vec{R}_i = 2\vec{\mu}_i a_0^{-3}(\varepsilon - 1)/(2\varepsilon + 1)$, being dependent on relevant solute state dipole moments $\vec{\mu}_i$ and the static dielectric constant of the solvent. Compared to PTNA, DPIPQ is characterized by evidently larger excited state dipole moment (Figure 4), thus defining relatively stronger solvatochromic shifts of the excitation or emission energies as well as larger changes in the range separation upon the solvent polarity. For this reason eventual solvation correction to the exchange screening parameter, which rises with the solvent polarity, is expected to be especially substantial for the CT states due to the fact that such states are usually characterized by large dipole moments.

4. CONCLUSIONS

We have reported here the absorption and fluorescence properties of organic compounds DPIPQ and PTNA calculated by the LC-BLYP DFT/TDDFT method in the PCM approach. These dyes represent five- and seven-membered heterocyclic isomers, respectively, i.e., molecules of similar sizes but considerably different chemical structures. The purpose of present work was to explore how such structural isomerization influences the range separation in long-range-corrected DFT/TDDFT/PCM analysis. The results of calculations are compared with the optical absorption and fluorescence spectra

dx.doi.org/10.1021/jp300305j | J. Phys. Chem. A 2012, 116, 3048−3055

measured in several organic solvents of different polarity. Despite a considerable structural difference, both dyes exhibit quite similar range separations, although it appears to be somewhat different for the optical absorption ($S_0 \rightarrow S_1$ transition, $\omega \sim 0.14-0.15$ Bohr^{-1}) and the fluorescence emission ($S_1^* \rightarrow S_0^*$ transition, $\omega \sim 0.21-0.23$ Bohr^{-1}) processes. In other words, stronger modification of the range separation is evidently required if one switches from the optical absorption to the fluorescence emission or vice versa. This finding is somewhat surprising taking into account that conformational relaxation in the excited state of both dyes leads to the structural changes being irrelevant with the ones corresponding to an isomeric modification. Nevertheless, properly parametrized LC-BLYP xc-potential reasonably predicts the excitation energies and oscillator strengths, including the electronic transitions to higher excited states; thus, basic features of the optical absorption spectra for both dyes may be well reproduced. In all the cases, DFT/TDDFT/PCM analysis predicts the blue shift of the first absorption band and the red shift of the fluorescence band on the rising solvent polarity F, i.e., in accordance with the experimental observation. However, the absolute values of the solvatochromic shifts appear evidently underestimated in most cases, especially for the fluorescence emission energy. Among the possible reasons for such discrepancy we consider the evaluated ground and excited state dipole moments, which are expected to be underestimated in DFT/TDDFT calculations using the LC-BLYP xc-potential. An alternative explanation considers a correction to the range separation caused by the solvent effect on the solute electron density. It turns out that the corresponding correction depends on the solvent polarity and is larger for the DPIPQ molecule, which in comparison to the PTNA dye, is characterized by a relatively larger excited state dipole moment. Accordingly, the origin of the solvent modified range separation is assumed to be related to the Onsager reaction field. For this reason it is expected to be especially important in the case of CT states usually characterized by large state dipole moments. Further experiments and long-range-corrected DFT/TDDFT/PCM analysis on relevant molecular systems are required to prove such an assumption.

AUTHOR INFORMATION

Corresponding Author

*E-mail: kityk@ap.univie.ac.at.

Notes

The authors declare no competing financial interest.

ACKNOWLEDGMENTS

This work have been prepared during author's stay (July-October 2011) at the Department of Experimental Physics (Saarland University, D-66041 Saarbrücken, Germany) and was supported by funding of this university. The author expresses his gratitude to all colleagues at the Department of Experimental Physics for kind hospitality. The DFT/TDDFT calculations have been carried out in Wrocław Centre for Networking and Supercomputing (http://www.wcss.wroc.pl), Grant No. 160.

REFERENCES

(1) Yamashita, Y. *Sci. Technol. Adv. Mater.* **2009**, *10*, 024313.
(2) Hasegawa, T.; Takeya, J. *Sci. Technol. Adv. Mater.* **2009**, *10*, 024314.
(3) Mao, G.; Orita, A.; Fenenko, L.; Yahiro, M.; Adachi, C.; Otera, J. *Mater. Chem. Phys.* **2009**, *115*, 378.
(4) Całus, S.; Gondek, E.; Danel, A.; Jarosz, B.; Pokladko, M.; Kityk, A. V. *Mater. Lett.* **2007**, *61*, 3292.
(5) Gondek, E.; Całus, S.; Danel, A.; Kityk, A. V. *Spectrochim. Acta, Part A.* **2008**, *69*, 22.
(6) Gondek, E.; Danel, A.; Kwiecień, B.; Sanetra, J.; Mac, M.; Kityk, A. V. *J. Mater. Sci.: Mater. Electron.* **2011**, *22*, 101.
(7) Gąsiorski, P.; Gondek, E.; Pokladko-Kowar, M.; Danel, K. S.; Matusiewicz, M.; Kuźnik, W.; Kityk, A. V. *Opt. Mater.* **2011**, *34*, 317.
(8) Lane, P. A.; Kafafi, Z. H. Solid-state organic photovoltaics: a review of molecular and polymeric devices. In *Organic Photovoltaics: Mechanisms, Materials, and Devices*; Sun, S., Sariciftci, N. S., Eds.; CRC Press: Boca Raton, FL, 2005; pp 49−104.
(9) Gondek, E.; Kityk, I. V.; Danel, A. *Mater. Chem. Phys.* **2008**, *112*, 301.
(10) Speiser, S.; Shakkour, N. *Appl. Phys. B: Laser Opt.* **1985**, *38*, 191.
(11) Tu, J.; Li, N.; Chi, Y.; Qu, S.; Wang, C.; Yuan, Q.; Li, X.; Qiu, S. *Mater. Chem. Phys.* **2009**, *118*, 273.
(12) Koścień, E.; Sanetra, J.; Gondek, E.; Danel, A.; Wisła, A.; Kityk, A. V. *Opt. Commun.* **2003**, *227*, 115.
(13) Całus, S.; Gondek, E.; Danel, A.; Jarosz, B.; Kityk, A. V. *Opt. Commun.* **2006**, *268*, 64.
(14) Całus, S.; Gondek, E.; Danel, A.; Jarosz, B.; Kityk, A. V. *Opt. Commun.* **2007**, *271*, 16.
(15) Całus, S.; Gondek, E.; Pokladko, M.; Kulig, E.; Jarosz, B.; Kityk, A. V. *Spectrochim. Acta, Part A.* **2007**, *67*, 1007.
(16) Wong, B. M.; Piacenza, M.; Salab, F. D. *Phys. Chem. Chem. Phys.* **2009**, *11*, 4498.
(17) Wong, B. M.; Hsieh, T. H. *J. Chem. Theory Comput.* **2010**, *6*, 3704.
(18) Praveen, P. L.; Ojha, D. P. *Cryst. Res. Technol.* **2012**, *47*, 91.
(19) Praveen, P. L.; Ojha, D. P. *Phys. Rev. E.* **2011**, *83*, 051710.
(20) Danel, K. S.; Wisła, A.; Uchacz, T. *ARKIVOC* **2009**, *x*, 71.
(21) Danel, K. S.; Gąsiorski, P.; Matusiewicz, M.; Całus, S.; Uchacz, T.; Kityk, A. V. *Spectrochim. Acta, Part A* **2010**, *77*, 16.
(22) Całus, S.; Danel, K. S.; Uchacz, T.; Kityk, A. V. *Mater. Chem. Phys.* **2010**, *121*, 477.
(23) Gąsiorski, P.; Danel, K. S.; Matusiewicz, M.; Uchacz, T.; Kityk, A. V. *J. Lumin.* **2010**, *130*, 2460.
(24) Gąsiorski, P.; Danel, K. S.; Matusiewicz, M.; Uchacz, T.; Vlokh, R.; Kityk, A. V. *J. Fluoresc.* **2011**, *21*, 443.
(25) Sato, Y.; Mizoguchi, T.; Kudo, Y.; Ishida, R. Novel triazafluoranthene compound and processes for preparing the same. U.S. Patent 4,367,230. *Chem. Abstr.* **1981**, *96*, 217867.
(26) Asselin, A. A.; Humber, L. G. 10b-Azafluoranthene derivatives and precursors thereof. U.S. Patent 4,171,443. *Chem. Abstr.* **1979**, *92*, 41918.
(27) Khan, S. I.; Nimrod, A. C.; Mehrpooya, M.; Nitiss, J. L.; Walker, L. A.; Clark, A. M. *Antimicrob. Agents Chemother.* **2002**, *46*, 1785.
(28) Wamberg, M. C.; Hassan, A. A.; Bond, A. D.; Pedersen, E. B. *Tetrahedron.* **2006**, *62*, 11187.
(29) Gąsiorski, P.; Danel, K. S.; Matusiewicz, M.; Uchacz, T.; Kityk, A. V. *Dyes Pigments* **2012**, *93*, 1538.
(30) Koścień, E.; Gondek, E.; Pokladko, M.; Jarosz, B.; Vlokh, R. O.; Kityk, A. V. *Mater. Chem. Phys.* **2009**, *114*, 860.
(31) Gondek, E.; Danel, A.; Kwiecień, B.; Nizioł, J.; Kityk, A. V. *Mater. Chem. Phys.* **2010**, *119*, 140.
(32) Koścień, E.; Gondek, E.; Jarosz, B.; Danel, A.; Nizioł, J.; Kityk, A. V. *Spectrochim. Acta, Part A.* **2009**, *72*, 582.
(33) Gąsiorski, P.; Danel, K. S.; Matusiewicz, M.; Uchacz, T.; Kuźnik, W.; Kityk, A. V. *J. Fluoresc.* **2012**, *22*, 81.
(34) Gąsiorski, P.; Danel, K. S.; Matusiewicz, M.; Uchacz, T.; Kuźnik, W.; Piatek, Ł.; Kityk, A. V. *Mater. Chem. Phys.* **2012**, *132*, 330.
(35) Kurashige, Y.; Nakajima, T.; Kurashige, S.; Hirao, K.; Nishikitani, Y. *J. Phys. Chem. A.* **2007**, *111*, 5544.
(36) Dreuw, A.; Head-Gordon, M. *J. Am. Chem. Soc.* **2004**, *126*, 4007.
(37) Wodrich, M. D.; Corminboeuf, C.; Schreiner, P. R.; Fokin, A. A.; Schleyer, P.v.R. *Org. Lett.* **2007**, *9*, 1851.

(38) Savin, A. *Recent Developments and Applications of Modern Density Functional Theory*; Elsevier: Amsterdam, 1996.
(39) Gill, P. M. W. *Mol. Phys.* **1996**, *88*, 1005.
(40) Leininger, T.; Stoll, H.; Werner, H. J.; Savin, A. *Chem. Phys. Lett.* **1997**, *275*, 151.
(41) Iikura, H.; Tsuneda, T.; Yanai, T.; Hirao, K. *J. Chem. Phys.* **2001**, *115*, 3540.
(42) Tawada, Y.; Tsuneda, T.; Yanagisawa, S.; Yanai, T.; Hirao, K. *J. Chem. Phys.* **2004**, *120*, 8425.
(43) Kamiya, M.; Sekino, H.; Tsuneda, T.; Hirao, K. *J. Chem. Phys.* **2005**, *122*, 234111.
(44) Sato, T.; Tsuneda, T.; Hirao, K. *Mol. Phys.* **2005**, *103*, 1151.
(45) Sato, T.; Tsuneda, T.; Hirao, K. *J. Chem. Phys.* **2007**, *126*, 234114.
(46) Vydrov, O. A.; Heyd, J.; Krukau, A. V.; Scuseria, G. E. *J. Chem. Phys.* **2006**, *125*, 074106.
(47) Krukau, A. V.; Vydrov, O. A.; Izmaylov, A. F.; Scuseria, G. E. *J. Chem. Phys.* **2006**, *125*, 224106.
(48) Vydrov, O. A.; Scuseria, G. E. *J. Chem. Phys.* **2006**, *125*, 234109.
(49) Rohrdanz, M. A.; Martins, K. M.; Herbert, J. M. *J. Chem. Phys.* **2009**, *130*, 054112.
(50) Baer, R.; Livshits, E.; Neuhauser, D. *Chem. Phys.* **2006**, *329*, 266.
(51) Livshits, E.; Baer, R. *Phys. Chem. Chem. Phys.* **2007**, *9*, 2932.
(52) Krukau, A. V.; Scuseria, G. E.; Perdew, J. P.; Savin, A. *J. Chem. Phys.* **2008**, *129*, 124103.
(53) Rohrdanz, M. A.; Herbert, J. M. *J. Chem. Phys.* **2008**, *129*, 034107.
(54) Lee, C.; Yang, W.; Parr, R. G. *Phys. Rev. B* **1988**, *37*, 785.
(55) Becke, A. D. *Phys. Rev. A* **1988**, *38*, 3098.
(56) Frisch, M. J.; Trucks, G. W.; Schlegel, H. B.;et al. *Gaussian 09*, revision B.01; Gaussian, Inc.: Wallingford, CT, 2010.
(57) Lippert, E. *Z. Naturforsch.* **1955**, *A10*, 541.
(58) Mataga, N.; Kaifu, Y.; Koizumi, M. *Bull. Chem. Soc. Jpn.* **1955**, *28*, 690.
(59) McRae, E. G. *J. Phys. Chem.* **1957**, *61*, 562.
(60) Wong, B. M.; Cordaro, J. G. *J. Chem. Phys.* **2008**, *129*, 214703.
(61) Balanay, M. P.; Lee, S. H.; Yu, S. C.; Kim, D. H. *Bull. Korean Chem. Soc.* **2011**, *32*, 705.
(62) Balanay, M. P.; Kim, D. H. *J. Phys. Chem. C* **2011**, *115*, 19424.
(63) Onsager, L. *J. Am. Chem. Soc.* **1936**, *58*, 1486.